Ab initio study on the low-lying excited states of retinal

Manuela Merchán and Remedios González-Luque
Departamento de Química Física, Universitat de València, Dr. Moliner 50, Burjassot, E-46100 Valencia, Spain

(Received 3 June 1996; accepted 11 October 1996)

Ab initio results for the electronic spectrum of *all-trans*-retinal and its truncated model 3-methyl-*all-trans* (10-*s*-*cis*)-2,4,6,8,10-undecapentaen-1-al are presented. The study includes geometry determination of the ground state. Vertical excitation energies have been computed using multiconfigurational second-order perturbation theory through the CASPT2 formalism. The lowest singlet excited state in gas phase is predicted to be of $n\pi^*$ character. The lowest triplet state corresponds, however, to a $\pi\pi^*$ state. The most intense feature of the spectrum is due to the strongly dipole-allowed $\pi\pi^*$ transition, in accordance with the observed maximum in the one-photon spectra. The vertical excitation energies of the B_u- and A_g-like states are found close, the latter ≈ 1 eV higher than the maximum in the two-photon spectra. Solvent effects and nonvertical nature of the observed maximum in the two-photon spectra are invoked in rationalizing the deviation with respect to the best present estimate for the A_g-like state. In addition, qualitative aspects of the one-bond photoisomerization about the $C_{11}=C_{12}$ double bond of retinal are considered. The overall isomerization picture from 11-*cis* into *all-trans*-retinal, as taking place mainly along the triplet manifold, agrees with experimental evidence. © *1996 American Institute of Physics.* [S0021-9606(97)01803-5]

I. INTRODUCTION

A retinyl chromophore is a common feature of a biologically important class of proteins known as rhodopsins (Rh). They are key proteins in vision and bacterial photosynthetic and phototactic functions.[1–4]

In most cases the chromophore of visual Rh is 11-*cis*-retinal, which is attached to opsin in a Schiff base linkage through an amino group of lysine. Upon the absorption of light, the chromophore undergoes a series of changes accompanying visual transduction. Bovine Rh is one of the most extensively studied systems. That irradiation of bovine Rh isomerizes the 11-*cis*-retinal chromophore to *all-trans* was already established in the late 1960s.[5] In the primary photochemical event of vision, the isomerization process generates a bathochromically shifted photoproduct, photo-Rh, with a highly distorted *trans* conformation. The isomerization process is essentially complete in 200 fs.[6] The thermally relaxed product of photo-Rh is subsequently formed, batho-Rh, with a distorted *all-trans* structure. The protein continues its thermal relaxation to give further intermediates,[7] leading eventually to the *all-trans*-retinal and the apoprotein opsin.[8] Since the originally orange-colored Rh becomes nearly colorless at this stage, the whole process is called bleaching. The *all-trans*-retinal is then reduced to retinol (vitamin A), esterified, isomerized to 11-*cis*-retinol, which is oxidized to 11-*cis*-retinal, and recombines with opsin to produce Rh. The *all-trans*-retinal to 11-*cis* isomerization occurs in retinochrome, generating 11-*cis*-retinal to be used by rhodopsin. Details of many of the crucial steps are still unknown. Understanding electronic changes associated with excited-state chromophore isomerization in these compounds is, therefore, a problem of fundamental importance. In particular, to understand the initial process of visual excitation on theoretical grounds, elucidating the mechanism of *cis–trans* isomerization of retinal combined with opsin is necessary. As a first step towards a theoretical study of this important photoisomerization reaction, results for the low-lying excited states of retinal are examined in the present contribution. As far as we are aware, the study represents the first fully correlated *ab initio* determination of the electronic spectrum of retinal and its isomerization.

Retinal has been investigated in great detail by many workers. Reviews covering different aspects of the problem are available in the literature.[1–4] The absorption spectra of retinals are characterized by three bands.[1,9] The principal absorption band, which is broad and diffuse, even when recorded in a low-temperature matrix, has a maximum around 3.3 eV (in hexane at room temperature). The two additional transitions at ≈ 4.4 and ≈ 5 eV are weaker. The isomer dependence of oscillator strengths has been analyzed.[10] The synthesis and several spectroscopic properties of all 16 isomers of retinal have been recently reported.[11] The *all-trans*-retinal (ATR hereafter) has probably been the isomer more extensively investigated both experimentally and theoretically.

Considering the molecular structure of ATR [see Fig. 1(a)], the nature of the low-lying excited states of the system can be expected to resemble that of long polyenes, maintaining certain features intrinsic to aldehydes.

Although retinal belongs to the C_1 point group, the excited states are usually classified in terms of the idealized C_{2h} point group of even polyenes. The two lowest singlet transitions in polyenes correspond to the $1\,^1B_u$ and $2\,^1A_g$ states, which lie within a small energy interval.[12,13] The transition to the $1\,^1B_u$ state is the most important feature of the polyenes spectra; the intensity increases with the carbon chain length. The $1\,^1B_u$ state is mainly described by a one-

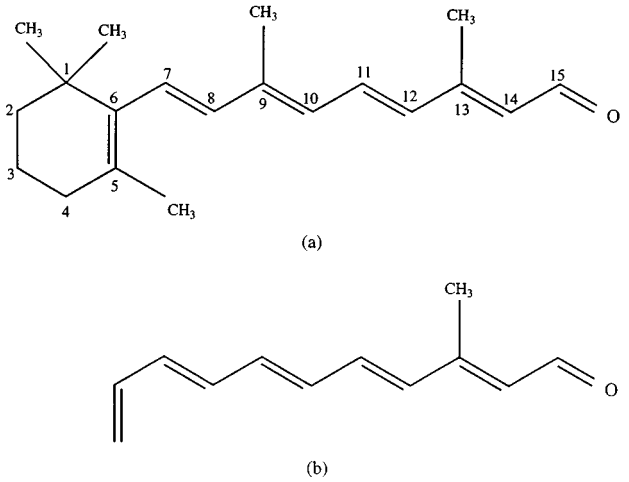

FIG. 1. (a) *All-trans*-retinal atom labeling; (b) truncated model employed, 3-methyl-*all-trans*(10-*s-cis*)-2, 4, 6, 8, 10-undecapentaen-1-al.

electron promotion from the highest occupied molecular orbital (HOMO) to the lowest unoccupied molecular orbital (LUMO). It has therefore an ''ionic'' character (in terms of valence bond structures). The nature of the electric-dipole forbidden $2\,^1A_g$ state is however ''covalent,'' with multiconfigurational character, involving a nonnegligible contribution from doubly excited configurations. Due to the presence of the carbonyl group, an additional low-lying $n\pi^*$ must also be assumed for retinal isomers. Based on previous studies on formaldehyde and acetone,[14,15] the state is expected to be described mainly by a single excitation from a lone-pair orbital of the heteroatom to a π^* orbital. For many years, the excited singlet manifold of retinal has provided a challenging system and the relative ordering of the low-lying states has been matter of controversy. The three lowest singlet excited states are expected to lie very close in energy. The relative ordering has been experimentally evidenced to be solvent dependent.[16,17] It is currently accepted, for instance, that the lowest excited singlet state of free ATR is of $n\pi^*$ character, while for the hydrogen-bonded retinal molecule it is of $\pi\pi^*$ nature and analog to the polyene $2\,^1A_g$ state. Picosecond time-resolved fluorescence experiments on ATR in hexane have recently revealed the existence of two fluorescent singlet excited states.[18] The photoexcitation first produces the optically allowed S_2 state (B_u-like), which relaxes to the optically forbidden S_1 state (A_g or $n\pi^*$) within 1 ps. The fast and slow fluorescence components have been assigned to the S_2 and S_1 states, respectively. However, the nature of the S_1 state could not be determined in this experiment.

The maximum of the most intense band in ATR is solvent and temperature dependent.[16,17,19] It has been located at 3.20 eV in EPA at 77 K,[20] at 3.31 and 3.37 eV in methanol and in hexane at 5°C,[21] and at 3.55 eV for retinal crystals.[22–24] On the other hand, the ^1A_g-like state has been placed at 2.95 eV in ATR crystal[23] and at 2.90 eV in solution (EPA, 77 K) by two-photon spectroscopy.[20] No direct experimental estimate on the $n\pi^*$ state is available. The study of the lowest triplet state has been hampered by the absence of phosphorescence. Raubach and Guzzo concluded from a singlet–triplet absorption spectrum of ATR that the lowest triplet state lies 1.54 eV above S_0.[25] Knowledge about the electronic nature of T_1 has been obtained by electron spin echo[26,27] and Raman[28,29] spectroscopies. These studies have concluded that the lowest triplet state of ATR is of $\pi\pi^*$ character. The electronic structure behaves as a polyenal containing six double bonds, which demonstrates that in the triplet state the double bond of the cyclohexene ring is part of the π-electron system. These findings give support to consider 2,4,6,8,10-undecapentaen-1-al (UND hereafter) and its methyl substituted systems as reasonable model compounds for the ATR molecule. Spectroscopic data on UND are also available.[30,31]

The role of the low-lying excited states in the photoisomerization reaction has been experimentally and theoretically analyzed. The 11-*cis* into *all-trans* ''one-way'' isomerization takes place predominantly in the triplet manifold.[4,32] Many spectroscopic studies have therefore focused on isomerization via the excited triplet state.[28,33–38] In the case of *all-trans* into *cis*, isomerization on a excited singlet surface might, however, be important.[18] Theoretical studies on the spectroscopy of retinals have been carried out with semiempirical methods.[1–4,20,39,40] It is worth mentioning that semiempirical calculations have predicted the lowest singlet to be of $n\pi^*$ character (see, e.g., Refs. 20,40). The present study confirms these earlier theoretical results.

We report in this paper results from *ab initio* calculations on the low-lying singlet and triplet excited states of *all-trans*-retinal and its truncated model 3-methyl-*all-trans*(10-*s-cis*)-2,4,6,8,10-undecapentaen-1-al [MUND hereafter, see Fig. 1(b)]. The study includes geometry determination of the ground state. In addition, the potential energy curves for the ground and low-lying excited states have been built with respect to the 11-*cis* into *all-trans*-retinal isomerization reaction coordinate. The most important reorganization and correlation effects in the valence shell are accounted for by using the CASSCF method.[41] The remaining correlation contributions are considered within the framework of multiconfigurational second-order perturbation theory, the CASPT2 approach.[42,43] The successful performance of the CASPT2 method in computing differential correlation effects for excitation energies has been illustrated in a number of earlier applications.[44,45] Particularly relevant to the present study are probably the investigations carried out on polyenes (ethylene, butadiene, hexatriene, and octatetraene),[12,13,46] studies on the spectroscopy of the carbonyl group (formaldehyde and acetone),[14,15] as well as determination of the electronic spectrum of norbornadiene.[47]

II. METHODS AND COMPUTATIONAL DETAILS

Full geometry optimizations were carried out at the Hartree–Fock (HF) level using the 3-21G basis set, the valence contraction of the $(9s5p)$ Dunning primitive set $(D95V)$, and including in the latter polarization functions on the carbon and oxygen atoms, hereafter called $D95Vd$. The largest calculation on the retinal system comprised 371 basis

TABLE I. CASSCF wave functions (number of active orbitals[a]) (number of active electrons) employed to compute the considered transitions of retinal, $C_{20}H_{28}O$, and 3-methyl-*all-trans*(10-*s-cis*)-2, 4, 6, 8, 10-undecapentaen-1-al, $C_{12}H_{14}O$.

Wave function	States	No. conf.[b]	N_{states}[c]
$C_{20}H_{28}O$ (C_1 symmetry)			
CASSCF(11)(14)	S_0, S_1, S_2, S_3, S_4	32 670	5
	T_1, T_2	50 820	2
$C_{12}H_{14}C$ (C_s symmetry)			
CASSCF(0-12)(12)	$1\,^1A', 2\,^1A', 3\,^1A', 4\,^1A'$	226 512	4
CASSCF(0-12)(12)	$1\,^3A'$	382 239	1
CASSCF(1-10)(14)	$1\,^1A''$	13 860	1
CASSCF(1-10)(14)	$1\,^3A''$	23 100	1

[a]Within parentheses the number of active orbitals of symmetry $a'-a''$ of the point group C_s.
[b]Number of configurations in the CASSCF wave function.
[c]States included in the average CASSCF calculation.

functions with 141 degrees of freedom. An average of 8 h per cycle were required on a IBM RISC 6000/590 computer and around 15 cycles were needed to complete a geometry optimization. The direct SCF algorithms implemented in the GAUSSIAN 94 package of programs were employed, using default criteria in all the cases.[48]

The low-lying states of the considered systems were computed using multiconfigurational second-order perturbation theory through the CASPT2 method.[42,43] The reference functions in the second-order perturbation treatment of each state were determined using the complete active space SCF (CASSCF) procedure.[41] Orbital relaxation and static correlation effects are included at this level. The CASPT2 calculations were performed using the full Fock matrix representation of the zeroth order Hamiltonian.[43] The energy of each excited state is referred to a ground-state energy computed with the same active space. All electrons except the cores were correlated.

The molecular orbitals for the excited states have been obtained from state average CASSCF calculations, where the averaging includes all states of interest of a given symmetry. The number of states included in the state average CASSCF calculations, together with the number of configurations in the CASSCF wave function, details on the active spaces used, and the type of states computed are given in Table I. The selection of the active spaces is determined by the type of states to be studied. In the present case the low-lying singlet and triplet valence states. In certain cases the active space had to be enlarged in order to avoid intruder state problems in the CASPT2 treatment.[45,49]

The transition dipole moments were computed by means of the CASSCF state interaction (CASSI) method.[50,51] In the formula of the oscillator strength the excitation energy computed at the CASPT2 level was employed.[44,45]

In the CASSCF/CASPT2 calculations generally contracted basis sets of the atomic natural orbital (ANO-S) type were used, which were obtained from the C,O $(10s6p3d)/\mathrm{H}(7s)$ primitive sets.[52] The contractions $\mathrm{C,O}[2s1p]/\mathrm{H}[1s]$ and $\mathrm{C,O}[3s2p1d]/\mathrm{H}[2s]$ were used in the present study.

The CASSCF/CASPT2 and CASSI calculations were performed using the MOLCAS-3 quantum chemistry software.[53]

III. RESULTS AND DISCUSSION

In this section we shall present and discuss the results for ATR and its truncated model MUND. The present findings will be compared with previous theoretical results and available experimental data. Such a comparison has to be seen with caution. On the one hand, experimental results were measured either in solution or in retinal crystal, whereas the theoretical results should be compared to observed gas-phase data. The positions of the low-lying excited states of ATR strongly depend on the environment. Our excitation energies are calculated for vertical transitions. Therefore, when possible, we compare the computed results with the Franck–Condon maxima observed for the corresponding bands. Exceptions, where the band maxima cannot be related to the vertical transition are, however, known. The difference of the vertical excitation and 0–0 transition energies is substantial for most of the bands considered here. These factors should be borne in mind when judging the accuracy of the calculations. On the other hand, doubtless due to the large molecular size, previous theoretical studies of the excited states of retinal were performed by using semi-empirical approaches, employing different parametrizations and degree of flexibility to describe the wave functions. Owing to the inherent characteristics of the semi-empirical methods, comparison with the *ab initio* treatment is not straightforward.

CASSCF wave functions have enough flexibility to describe all type of excited states, independent of their nature, valence, Rydberg, with singly or doubly excited character, etc., and the CASPT2 method gives accurate estimates of the relative dynamic correlation energy. The statement is supported by a number of studies, ranging from ethylene to free-base porphin. A properly chosen one-electron basis set has to be provided. Calibration calculations indicated that at least basis sets of split-valence plus polarization quality are required for a quantitative description of valence transitions.[54,55] For systems of the size of retinal, with C_1 symmetry, geometry optimizations at the HF level, even with inclusion of polarization functions, have currently become routine due to the development of efficient direct algorithms. Fully correlated calculations of ATR using extended one-electron basis sets are, however, beyond the limit of what present technology can handle. A minimal basis set was used in the analysis of the main spectral features of the ATR system. Such a calculation is not expected, of course, to yield accurate excitation energies but is able to show significant trends. Previous work has shown that in spite of the large errors associated to the small basis sets, there are many similarities between the results employing minimal and extended basis sets (see, e.g. Ref. 56). In particular, the study can give new insight to the electronic changes involved in the low-lying excited states during a *cis–trans* isomerization process of retinal. In addition, the study of the ATR system is required in order to analyze the possibility of using truncated

molecular models, where larger basis sets could be employed, yielding the usual accuracy in vertical transition energies (two-tenths of an eV). The truncated model used here is the MUND molecule. The difficulties associated to the *ab initio* study of a system of this molecular size have been clearly illustrated in the work by Du and Davidson on related molecules.[57]

Geometry determination of ground-state retinal is first considered. The vertical excitation energies of ATR and MUND are next analyzed. The photoisomerization of 11-*cis* to *trans* retinal is finally discussed.

A. Geometry determination of ground-state retinal

Characterization of the ground-state geometry of retinal to be employed in the spectroscopic study is presented in this section. We shall focus on the ATR system. A parallel study has been carried out for 11-*cis*(12-*s*-*trans*)retinal leading to similar conclusions.

The gas-phase molecular structure might in several geometric parameters deviate considerably from the crystal data due to puckering disorder.[58,59] The disorder originates from the rapid interconversion between two half-chair conformers.[60] The crystal data of this type of compounds are in general characterized by disorder of the β-ionone ring. It is evidenced in the ATR crystal structure for the short C_2-C_3 single bond distance of the cyclohexenyl ring. The disorder limits the possibility to determine internal torsion angles accurately. X-ray diffraction techniques may also lead to an artificial shortening of carbon–carbon bonds with higher π-bond electron order than neighboring bonds. In addition, the technique is not suited to locate the hydrogen nuclei. For these reasons, geometry optimization of ground-state ATR was initially undertaken. Computed vertical excitation energies in long polyenes like *all-trans*-1,3,5,7-octatetraene were found, using similar approaches, to be sensitive to the geometry employed for the ground state.[13] Thus an accurate determination of the gas-phase spectrum must be preceded by a geometry optimization of the ground state.

The *D*95*Vd* basis set was chosen for the HF geometry optimization in order to relate the accuracy of the present computed bond distances to the findings obtained in octatetraene. The optimized HF carbon–carbon single bonds in the polyene were about 0.004 Å longer than the CASSCF values (12 active π-orbitals, with the π-electrons active). The HF C=C optimal bond distances were, however, underestimated by 0.020 Å in octatetraene.[13] Similar trends can be expected for the ground-state parameters of ATR. To analyze the influence of polarization functions on the carbon and oxygen atoms, geometry optimization was also carried out employing the *D*95*V* basis set. Geometry optimization of ground-state ATR using the 3-21G basis set has been recently reported by de Lera and co-workers.[61] They obtained the skewed *s*-*cis* for the C_6-C_7 bond joining the cyclohexenyl ring to be the most stable conformation for ATR. Table II collects the computed bond distances and the dihedral angle between the plane of the ring and the chain using the 3-21G; *D*95*V*, and *D*95*Vd* basis sets. Full geometry optimization was performed in all the cases. For sake of comparison, the crystal data are also included.

TABLE II. Geometrical parameters for the ground state of the *all-trans*-retinal molecule computed at the HF level (full geometry optimization) using different basis sets. The crystal data for the selected parameters are also included.

Parameter[a]	3-21 G[b]	*D*95 *V*[c]	*D*95 *Vd*[d]	X-Ray[e]
$r(C_1-C_2)$	1.543	1.548	1.540	1.545
$r(C_1-C_6)$	1.539	1.547	1.542	1.535
$r(C_2-C_3)$	1.532	1.530	1.524	1.420
$r(C_3-C_4)$	1.533	1.530	1.524	1.494
$r(C_4-C_5)$	1.521	1.522	1.517	1.505
$r(C_5-C_6)$	1.328	1.346	1.338	1.330
$r(C_6-C_7)$	1.491	1.493	1.495	1.482
$r(C_7-C_8)$	1.325	1.340	1.332	1.315
$r(C_8-C_9)$	1.474	1.477	1.477	1.467
$r(C_9-C_{10})$	1.335	1.351	1.342	1.345
$r(C_{10}-C_{11})$	1.456	1.461	1.463	1.442
$r(C_{11}-C_{12})$	1.331	1.345	1.338	1.338
$r(C_{12}-C_{13})$	1.469	1.473	1.474	1.452
$r(C_{13}-C_{14})$	1.334	1.351	1.343	1.344
$r(C_{14}-C_{15})$	1.463	1.466	1.476	1.455
$r(C_1-C_{16})$	1.547	1.551	1.542	1.511
$r(C_1-C_{17})$	1.545	1.551	1.543	1.538
$r(C_5-C_{18})$	1.518	1.518	1.515	1.506
$r(C_9-C_{19})$	1.515	1.514	1.511	1.491
$r(C_{13}-C_{20})$	1.517	1.516	1.513	1.495
$r(C_{15}-O)$	1.215	1.228	1.197	1.200
$\angle(C_5C_6C_7C_8)$	67.97	59.11	64.11	62

[a]Bond distances in Å and dihedral angle in degrees. See Fig. 1(a) for atom labeling.
[b]Total energy: −843.744 648 a.u. (245 basis functions). See also Ref. 61.
[c]Total energy: −848.208 977 a.u. (245 basis functions).
[d]Total energy: −848.578 113 a.u. (371 basis functions).
[e]Crystal data taken from Ref. 59.

The x-ray value 1.420 Å for the single bond distance C_2-C_3 is definitely too short. The conclusion is independent of the basis set employed. The computed results are more in accordance with the assumed bond distance for cyclohexene in gas phase.[62] A longer bond distance, 1.498 Å, was determined in the crystal structure of 11-*cis*-retinal, where the β-ionone ring exhibits less amount of disorder.[58] A detailed comparison of the *D*95*Vd* results with the crystal data shows the computed C–C single bonds for the polyene chain to be longer than in the crystal. Smaller deviations are found for the double bonds, except for the $C_5=C_6$ and $C_7=C_8$ bond distances. Based on the trends found in octatetraene, inclusion of π-valence correlation in the optimization procedure should decrease the C–C bond distances of the polyene backbone, making a better agreement with the crystal characterization. The C=C bond lengths should, however, increase, resulting in even larger deviations with respect to the crystal data when the π-valence correlation contributions were considered. It is therefore concluded that the measured $C_5=C_6$ (1.330 Å) and $C_7=C_8$ (1.315 Å) bonds are too short (1.339 Å in ethylene, see discussion in Ref. 13).

With the three basis sets employed, the gas-phase molecular structure of ground-state ATR displays a *trans* geometry and forms a nearly planar polyene chain with a 6-*s*-*cis*-conformation rotated 59°–68° from the idealized planar

s-cis arrangement. The polyene chain shows the expected bond alternation and decreases in the alternative character of the single and double bonds towards the center of the molecule, the so called size effect. The energetic balance among the different covalent and ionic structures (in the valence bond sense) strongly depends on the details of the basis sets employed. They lead ultimately to pronounced differences in the computed bond distances. Compared to the most extended basis set used ($D95Vd$), the results computed using the valence basis sets 3-21G and $D95V$ yield, in general, too short and too long bonding distances, respectively. Polarization functions do affect the calculated bond distances. They are also expected to be important to properly describe the bond and dihedral angles. Unless otherwise stated, the geometry derived from the HF full geometry optimization using the $D95Vd$ basis set has been used throughout. The bond distances at this level are expected to be within ± 0.01 Å of the actual gas-phase structure.

A parallel study has been performed to the 11-*cis*(12-*s-trans*)retinal system. The total energy, from the full geometry optimization HF procedure, of the 11-*cis* isomer turns out to be 0.269 eV (3-21G), 0.252 eV ($D95V$), and 0.264 eV ($D95Vd$) above the corresponding minima of the *all-trans* structure. The relative stability between the two rotamers, computed at the HF level, is thus not sensitive to the basis set employed.

B. Vertical excitation energies

The low-lying singlet and triplet vertical transitions have been computed, using the optimal HF geometry for the ground state of the ATR molecule obtained with the $D95Vd$ basis set. The C,O$[2s1p]$/H$[1s]$ ANO-S type basis set has been used in the calculation of the spectral properties. The number of roots in the average CASSCF calculation was systematically increased for the singlet states to reach the expected intense transition to the $\pi\pi^*$ state. Not until the number of roots was five the strong optically allowed transition was found. On the other hand, two lowest triplet states have been computed well below the nearest higher next triplet state. The study is therefore concentrated on the energy range up to the first strong dipole-allowed transition and on the two lowest triplet states. These states are expected to carry the relevant features for the understanding of the photoisomerization of retinal. Eleven active orbitals with 14 electrons have been employed for all the states. The selected active space enables a balanced treatment of the correlation effects taken into account variationally and perturbationally, reflected in the lack of intruder state problems in the CASPT2 step. The results for ATR are collected in Table III. The first column identifies the different states. The second and third columns give the vertical transition energies obtained by the CASSCF and CASPT2 calculations, respectively. In the remainder of the table, μ, the dipole moment computed at the CASSCF level (in Debye), and oscillator strengths are listed.

The calculated lowest vertical excitation energy for a singlet state appears in ATR at 3.36 eV as the $S_1(n\pi^*)$ state.

TABLE III. Computed excitation energies (in eV) and other properties of the vertical excited states of *all-trans*-retinal. The optimal ground-state HF/$D95Vd$ geometry was employed. The ANO-S type C,O$[2s1p]$/H$[1s]$ basis set was used in the spectral study. Within parentheses the results for a truncated model employing the same geometry and basis set (see the text).

State	CASSCF	CASPT2	μ[a]	Osc. Str.
Ground state (S_0)			3.186	
Singlet states				
$S_1(n\pi^*)$	3.46(3.57)	3.36(3.40)	1.321	0.000
$S_2(\pi\text{-}diex)$	6.00(5.92)	5.29(5.26)	5.992	0.130
$S_3(n\pi,\pi^*\pi^*)$	5.91	5.35	1.154	0.000
$S_4(\pi\pi^*)$	6.82(6.68)	5.78(5.96)	8.043	1.594
Triplet states				
$T_1(\pi\pi^*)$	3.45(3.25)	2.79(2.73)	3.441	
$T_2(n\pi^*)$	3.11(3.08)	2.89(2.94)	1.157	

[a]Dipole moment (CASSCF) in Debye.

It is partly described by a one-electron promotion from the lone pair of the heteroatom to the LUMO π orbital, which has a weight of 58% in the CASSCF wave function. The states implying excitations with the π system, are obtained, as expected with such a limited basis set, at too high energies. The second vertical state, denoted as $S_2(\pi\text{-diex})$, has a sizeable contribution (27%) of the doubly excited configuration from the HOMO to the LUMO. It has a computed intensity of 0.13. A extremely weak transition is found next. The main contribution to the S_3 state is due to a mixed-character double excitation $n\pi\rightarrow\pi^*\pi^*$ with a weight of 37%. The fourth singlet excited state corresponds to the $S_4(\pi\pi^*)$ state located at 5.78 eV, with a computed intensity of 1.6. The singly excited HOMO$\rightarrow$LUMO configuration contributes 52% in the CASSCF wave function. It is for the $S_4(\pi\pi^*)$ state where the difference between the excitation energies at the CASSCF and CASPT2 levels is the largest ($\approx$1 eV), according to its ionic nature. Larger basis sets with greater flexibility are certainly required for its quantitative description. The lowest triplet state, $T_1(\pi\pi^*)$, is of π character. The singly excited $\pi\rightarrow\pi^*$ configuration has a weight of 53% in the CASSCF wave function. The $T_2(n\pi^*)$ state is found energetically close, and is described by a CASSCF wave function in which the weight of the singly excited $n\rightarrow\pi^*$ configuration is 71%.

The MUND system, as model of the ATR molecule, has also been investigated at the same level (same basis set and active space as ATR). Several calibration calculations have been performed to check the effect of different geometries on the excitation energies of the truncated model compared to the ATR system. At the CASPT2 level, employing the optimized HF/$D95Vd$ geometry of ATR for the MUND molecule (results within parentheses in Table III), the T_1 and T_2 states are located at 2.73 and 2.94 eV, respectively. When the structure is forced to be planar (with the same bond lengths and bond angles of ATR), the excitation energies are computed to be 2.66 eV (T_1) and 2.98 eV (T_2). In addition, when the optimized HF geometry of MUND is employed ($D95Vd$ basis, data not shown) a further decrease takes place for the T_1 state, 2.60 eV, with no change for the T_2 state, computed at 2.98 eV. These values represent a devia-

TABLE IV. Computed excitation energies (in eV) and other properties of the vertical excited states of 3-methyl-*all-trans*(10-*s*-*cis*)-2,4,6,8,10-undecapentaen-1-al and for its isomer related to 11-*cis*(12-*s*-*trans*)retinal. The corresponding optimal ground-state HF/*D*95*Vd* geometry was employed. The ANO-S type C,O[3*s*2*p*1*d*]/H[2*s*] basis set was used in the spectral study.

State	CASSCF	CASPT2	μ^a	Osc. Str.
all-trans				
Ground state ($1^1A'$)			3.367	
Singlet states				
$1^1A''(n\pi^*)$	4.17	3.54	0.215	Forbidden
$2^1A'(\pi\pi^*)$	6.19	3.76	7.641	1.077
$3^1A'(\pi$-diex)	4.64	3.89	3.842	0.002
Triplet states				
$1^3A'(\pi\pi^*)$	2.56	1.96	3.573	
$1^3A''(n\pi^*)$	3.80	3.35	0.216	
cis				
Ground state ($1^1A'$)			3.483	
Singlet states				
$1^1A''(n\pi^*)$	4.01	3.61	0.397	Forbidden
$2^1A'(\pi\pi^*)$	6.15	3.81	7.459	0.966
$3^1A'(\pi$-diex)	4.62	3.87	3.634	0.000
Triplet states				
$1^3A'(\pi\pi^*)$	2.55	1.96	3.547	
$1^3A''(n\pi^*)$	3.77	3.33	0.282	

[a]Dipole moment (CASSCF) in Debye.

tion from ATR of -0.19 and 0.09 eV for the T_1 and T_2 states, respectively. Towards planarity the vertical excitation energy of the T_1 state has a more pronounced decrease, because the expected planarity of the triplet state makes the stabilization of the excited state larger than for the ground state. We conclude that MUND can be confidently used as reasonable model for ATR.

The actual optimal geometry of the MUND system belongs to the C_1 symmetry. However, the optimized geometry within the constraints of the C_s point group is isoenergetic (within 0.001 eV). It is not surprising since the polyene chain is nearly planar and the C_s restriction mainly affects to the methyl group. Within the C_s symmetry, using the corresponding optimized structure determined at the HF level with the *D*95*Vd* basis set, a study of the electronic spectrum was carried out with an extended basis set for the backbone. The ANO-S generally contracted basis set C,O[3*s*2*p*1*d*]/H[2*s*] (198 basis functions) was employed. The same active space as in ATR was used for the $n\pi^*$ states. It had to be enlarged, however, to 12 active orbitals, with 12 active electrons, for the $\pi\pi^*$ states in order to minimize the problem of intruder states in the CASPT2 calculation. An active space comprising all valence π orbitals is also the natural choice for a polyene chain. For the $\pi\pi^*$ states the lone pair of the heteroatom behaves as an inactive orbital. The occupation number is close to 2.0 when it is treated as active. In addition, when exciting out from the lone pair, the lowest π orbital can, to a good approximation, be treated as inactive. The highest unoccupied π orbitals have for this excitation a low occupation number and are moved to the virtual space. The calculated vertical excitation energies are compiled in Table IV.

The results for MUND give further support to assign the lowest singlet state of ATR to the $S_1(n\pi^*)$ state, calculated at 3.54 eV for the *all-trans* structure at the CASPT2 level. The result is only 0.10 eV larger than the corresponding minimal basis set result at the same level, employing the same geometry. This finding seems to point out to similar energetic correlation contributions on both the ground and the first excited state, which cancel each other in large extent. A reasonable description of the first excited state can be therefore achieved for ATR, in spite the limited basis set employed. The situation is different for the states of π character. The $2\,^1A'(\pi\pi^*)$ state is placed at 3.76 eV, with a computed oscillator strength of 1.1. The singly excited configuration HOMO→LUMO contributes 68% in the CASSCF wave function. Slightly above is found the $3\,^1A'(\pi$-diex) state, which corresponds to a weakly dipole-allowed transition. The main configurations describing the $3\,^1A'$ state are: HOMO→LUMO+1 (13%), HOMO−1→LUMO (15%), and HOMO,HOMO→LUMO,LUMO (28%). That is, the electronic structure of the state clearly resembles that of the corresponding A_g state of a polyene. On the other hand, the results on the triplet vertical excitation energies of the MUND system certainly confirm the $\pi\pi^*$ nature of the lowest triplet state, placed at 1.96 eV above the ground state. The $1\,^3A''(n\pi^*)$ state is computed to be more than 1 eV above the $1\,^3A'(\pi\pi^*)$ state.

The present results can be compared to the experimental information for the ATR system,[20–24] as well as the available data for UND.[30,31] In the one-photon spectra of ATR the maximum is located in the energy range 3.20–3.37 eV depending on the solvent[20,21] and at 3.55 eV for retinal crystal.[22–24] A similar situation was observed in UND.[31] Considering the expected bathochromic shift for the most intense transition in solution,[19] the best estimate vertical results, 3.76 eV, agree with the experimental data. A significant deviation ($\approx$1 eV) is, however, noted between the maximum observed in the two-photon spectra of ATR (at 2.90 eV) and the computed vertical transition for the $3\,^1A'(\pi$-diex) state in MUND (3.89 eV). For UND, which has the same number of double bonds like retinals, a low-lying weak transition has also been observed at a similar energy in both one-photon absorption and excitation spectra in different solvents.[31] The change of dipole moment from the ground state to the π-diex excited state is not so pronounced as in the case of the $\pi\pi^*$ state (cf. Table III and Table IV). One would therefore on this ground not expect a solvent redshift of 1 eV. It is, however, possible that other effects than the solvent are important for the difference between the spectrum of ATR (or MUND) in gas phase and solution. One possibility is a nonvertical nature of the observed transition.

In 1971 Raubach and Guzzo[25] located T_1 at 1.54 eV above S_0 for the ATR molecule (1.37 eV was observed for UND ten years earlier.[30] The lowest triplet state, vertically computed at 1.96 eV, is consistent with these experimental excitation energies, which were assigned to the 0–0 transition. A common feature, which has been obtained in a number of studies of *trans* polyenes, is related to the location of

the $2\,^1A_g$ state with respect to the lowest triplet, $1\,^3B_u$ state. The vertical excitation energy of the $2\,^1A_g$ state was found, within 0.1 eV, to be twice the vertical excitation energy of the HOMO→LUMO triplet state. It can be rationalized from the fact that the HOMO,HOMO→LUMO,LUMO configuration, important in the description of the $2\,^1A_g$ state, is the result of two singlet coupled triplet HOMO→LUMO excitations. For instance, at the CASPT2 level, the lowest valence $^3B_u(^1A_g)$ states are placed at 3.20(6.27), 2.55(5.20), 2.17(4.38) eV for *trans*-butadiene, *trans–trans*-hexatriene,[12] and *all-trans*-octatetraene,[13] respectively. A natural assumption is to assume that the same relation is fulfilled for the systems considered here. Twice the best estimate for $T_1(\pi\pi^*)$ in MUND, 1.96 eV, is only 0.03 eV larger than the actual computed value for the π-diex state (3.89 eV). We therefore conclude that the computed vertical transition for the π-diex state gives a reasonable gas-phase estimate. The large difference from the maximum observed in the two-photon absorption spectra in solution is most probably due to a nonvertical nature of the observed transition. Geometry relaxation of the excited state is expected to be of the same order as the deviation. It was computed to be 0.8 eV for the $2\,^1A_g$ state of octatetraene. It is also remarkable that for the same polyene the 0–0 transition to the $1\,^1B_u$ was only 0.1 eV below the corresponding vertical transition. Thus geometry relaxation of the π-diex excited state involves a larger energetic stabilization than for the $\pi\pi^*$ state. The main factor explaining the difference between the computed and experimental results for the optically allowed transition can be related to influence of the environment. For the π-diex state both geometry relaxation and solvent effects have to be taken into account.

As can be seen in Tables III and IV, the computed dipole moment for the intense optically allowed excited state is nearly twice the dipole moment of the ground state. The result of the $\pi\pi^*$ excited-state dipole moment, 8.0 for ATR and 7.6 D for MUND, gives support to the experimentally derived gas-phase value for retinal, 7 ± 1 D.[63] Ponder and Mathies also reported a solution-phase excited-state dipole moment of 19.8 ± 0.7 D. Thus the dipole moment of the excited state more than doubles upon solvation. These authors pointed out an implied unusually large reaction field factor due to the large excited-state polarizability of retinal.[63] On the other hand, the dipole moment for the $n\pi^*$ state is computed to be considerably less than that of the ground state with the components of opposite sign. It will create a repulsive interaction with the solvent leading to the expected solvation blueshift. Since the ground state dipole moment points toward the ionone ring, it indicates a shift of electrons from the aldehyde moiety in the $n\pi^*$ excited state. It is reflected on the population analysis performed with the CASSCF wave functions, where the oxygen atom bears a net charge of -0.313 in the ground state, compared to -0.170 electrons in the $n\pi^*$ state of ATR. The relative state ordering of the $n\pi^*$ state is likely to be strongly influenced by the type of the solvent as proposed by several authors.[16,17,19]

The description given by the semi-empirical methods depends on the details of the approach used. For instance, the all-valence-electron INDO-PSDCI calculations, employing the crystal determined geometry of ATR, predicted a low-lying $n\pi^*$ state at 3.28 eV nearly degenerate with the lowest π-diex state at 3.26 eV, which are slightly below the $\pi\pi^*$ state at 3.53 eV. The reverse trend, with a value 1 D larger for the π-diex state than for the $\pi\pi^*$ state ($\approx$8 D), for the dipole moments was obtained.[20] Accordingly, solvent polarity changes were expected to affect both states similarly.

Similar excitation energies and properties were found for the truncated model MUND of 11-*cis*(12-*s*-*trans*)retinal (cf. Table IV). The corresponding *cis* HF/*D*95*Vd* optimized geometry, located 0.23 eV above the MUND structure at this level, was employed in the spectral study. The same basis set, including up to *d*-type functions on the carbon and oxygen atoms, and the same active spaces were used. The $n\pi^*$ state, located at 3.61 eV, was computed to be the lowest singlet excited state. The present results confirm, therefore, the $n\pi^*$ nature of the lowest transition of dry retinals in dry nonhydrogen-bonding solvents.[2] The low-lying triplet states of the 11-*cis* isomer had similar transition energies and characteristics as the *trans* conformer with: $T_1(\pi\pi^*)$ at 1.96 eV and $T_2(n\pi^*)$ at 3.33 eV. The $n\pi^*$ nature of S_1 and the $\pi\pi^*$ character of T_1 are expected to have a substantial impact on the photophysical properties and photoisomerization characteristics of the 11-*cis* and *all-trans*-retinal.

C. Potential energy curves: 11-*cis*↔ *all-trans*-retinal isomerization

The aim of this part of the study is to obtain a qualitative understanding of the isomerization process taking place around the $C_{11}=C_{12}$ double bond of retinal. For this purpose the analysis have been performed at the CASSCF level, with the same active space, geometry, and basis set employed in the description of the vertical transitions of ATR. The importance of the second-order corrections have, however, been monitored at certain twisted angles. The qualitative nature of the conclusions (imposed from the beginning due to the limited basis set used) obtained with the CASSCF energies did not change at the CASPT2 level. Therefore, we mainly concentrate the discussion to the CASSCF results.

Potential energy curves with respect to the variation of the dihedral angle (Φ) defined between the planes $C_{13}–C_{12}–C_{11}$ and $C_{12}–C_{11}–C_{10}$ were built in 30° steps. A torsional angle $\Phi=0°$ corresponds to a 11-*cis*(12-*s*-*trans*)retinal. At 90° the 13-methyl is below the cyclohexenyl ring, with C_{13} closer to C_5 than at 270°. The remaining geometric parameters were fixed at the HF optimized structure of ATR [*all-trans* (6-*s*-*cis*)retinal,$\Phi=180°$], using the *D*95*Vd* basis set. The corresponding potential energy curves for the ground and the considered excited states are depicted in Fig. 2.

Inspection of the potential energy curves shows the symmetric nature between the 0°–180° and 180°–360° ranges of the dihedral angle Φ. In spite the nonequivalent molecular environment, steric repulsion effects affect in a similar way the studied states in both intervals. The potential curve for the S_0 state has a maximum at 90°. It is nearly isoenergetic

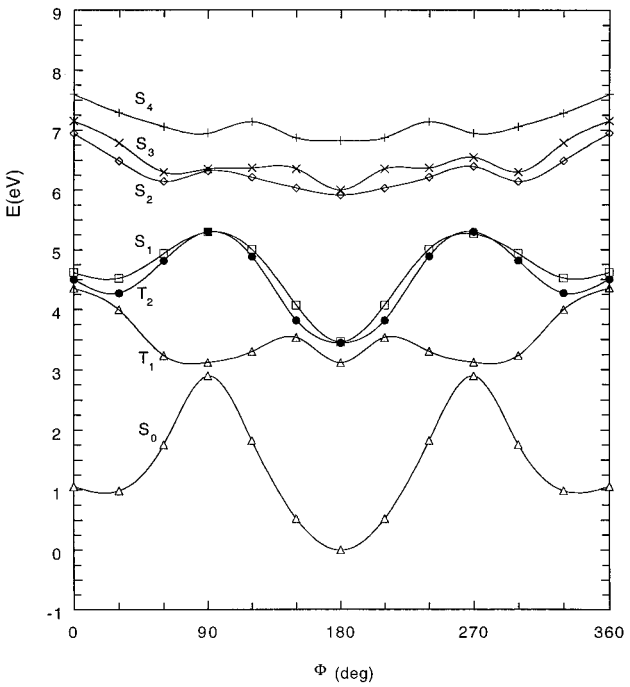

FIG. 2. Potential energy curves for rotation about the $C_{11}=C_{12}$ double bond in various states of retinal computed at the CASSCF level (11 active MOs/14 active electrons), using the C,O[2*s*1*p*]/H[1*s*] generally contracted ANO-type basis set. The optimal ground-state HF/*D*95*Vd* geometry for *all-trans*-retinal, obtained from the full optimization of the system, was employed throughout.

at this point with the T_1 state. At $\Phi=90°$, both S_0 and T_1 are of $\pi\pi^*$ character, with the CASSCF wave function described mainly by the HOMO→LUMO singly excited configuration. The potential energy curves for the singlet and triplet $n\pi^*$ states behave parallel and close to each other, with a maximum at 90°. The reason is the small overlap between the oxygen lone-pair and the π^* orbital. In a simple molecular orbital model, the relative stabilization of the triplet with respect to the corresponding singlet is given by the exchange integral, $K_{n\pi^*}$. Due to the poor overlap between the orbitals involved, the relative stabilization of the triplet is small. The $n-\pi^*$ overlap progressively decreases with the twisting, resulting in near degeneracy between the triplet and singlet $n\pi^*$ states at 90°. The upper states vary smoothly with respect to the torsional angle. For these states the computed dipole moments show larger variations along the reaction coordinate. The S_2 state at 90° is described mainly by the closed-shell Hartree–Fock configuration with a zwitterionic nature, which has a dipole moment of 14 D. It is clearly a case of ''sudden polarization.''[64]

For the general understanding of the shapes expected along the torsion of a double bond is helpful to recall the situation in ethylene. The *cis–trans* isomerization of olefines have received considerable attention by many different groups. Classic references to key studies can be found, for instance, in the book of Salem entitled ''Electrons in Chemical Reactions: First Principles'' published in 1982.[65] We shall only consider the basic aspects of the electronic changes associated to the *cis–trans* isomerization of the model system ethylene. In the simple two-electron two-orbital picture, the valence states of ethylene are ground $N=|\pi\overline{\pi}|$, lowest-triplet $T=|\pi\pi^*|$, lowest-valence singlet $V=|\pi\overline{\pi^*}|+|\pi^*\overline{\pi}|$ (apart from the normalization factor), and the doubly excited singlet $Z=|\pi^*\overline{\pi^*}|$. Twisted to 90° ethylene forms a diradical, dimethylene. In terms of the perpendicular atomic orbitals, denoted *a* and *b*, Mulliken demonstrated in 1932 the existence of four electronic states:[66] singlet diradical $^1D=|a\overline{b}|+|\overline{a}b|$, triplet diradical $^3D=|ab|$, and two zwitterionic states $^1Z(-)=|a\overline{a}|-|b\overline{b}|$ and $^1Z(+)=|a\overline{a}|+|b\overline{b}|$. Correlation between the states of the diradical and those of parent ethylene molecule is, however, complicated due to the presence of Rydberg states.[12] Without considering the possible avoided crossings, the following trends are present for the valence states. The *N* and *Z* configurations are degenerated at 90°. The minus and plus combinations give rise to the ^1D and $^1Z(+)$ states, respectively. Thus the ^1D state correlates with the ground state ethylene, the ^3D state originates from the *T* state of parent molecule, whereas the $^1Z(-)\leftrightarrow V$ and $^1Z(+)\leftrightarrow Z$ states are equally related. Resemble of these trends can be visualized along the $C_{11}=C_{12}$ twisting of retinal. At 90° the diradical S_0 and T_1 states and nearly degenerate, whereas the S_2, S_3, and S_4 states are shown at higher energies. Due to the localized nature of the HOMO and LUMO on the carbon atoms C_{11} and C_{12} at $\Phi=90°$, and 270°, together with the limited flexibility of the one-electron basis set, the CASPT2 relative energies with respect to S_0 are similar to that obtained at the CASSCF level. For instance, at $\Phi=90°$, the S_1,S_2,S_3, and S_4 states are located 2.40(2.29), 3.42(3.23), 3.45(3.30), 4.04(4.11) eV above S_0 at the CASSCF-(CASPT2) levels, respectively.

Retinal can be considered a prototype system undergoing to *cis–trans* isomerization and has been therefore extensively studied. We shall concentrate on the available information concerning the photoisomerization of 11-*cis*↔ *all-trans*-retinal. The 11-*cis* isomer exhibits a extremely rapid and efficient one-way isomerization into the *all-trans* species, while that from *trans* into 11-*cis* is much less efficient. The 11-*cis* to *trans* photoisomerization takes place predominantly in the triplet manifold. This fact has been shown by picosecond time-resolved absorption spectroscopy,[35] Raman spectroscopies,[33,37] and by determination of the quantum yields of triplet-sensitized isomerizations.[28,38] This unique isomerization property has been ascribed to the intrinsic structures of the 11-*cis* molecule and the *all-trans* T_1 species.[4] The structure of the latter has been deduced to be planar by Raman spectroscopy[28,29] and from electron-spin-echo studies.[26,27] The so-called ''triplet-excited region,'' about six conjugated double bonds long, detected by transient Raman spectroscopy[28] seems to determine the relative energies of the 11-*cis* and the *all-trans* isomers and to function as a driving force of isomerization in the T_1 manifold. The 11-*cis* conformation should be least advantageous in accommodating the triplet-excited region. The short lifetime of the 11-*cis* triplet together with the selective decay of the

11-*cis* triplet to the *all-trans* conformation have suggested a skewed torsional surface with no, or a small, barrier surrounding the 11-*cis* triplet.[34–36] Sensitized photoisomerization studies have concluded, on the other hand, that one-photon one-bond isomerizations are dominant.[38]

The computed potential energy curves and properties of the involved states are consistent with the current experimental picture. For the 11-*cis* isomer, transition to the $\pi\pi^*$ state will carry most of the excitation energy owing to its strongly allowed Franck–Condon character. In condensed phases a radiationless conversion from the $\pi\pi^*$ to the $S_1(n\pi^*)$ state can be expected to be extremely fast.[67] That the lowest singlet state has a $n\pi^*$ character plays a fundamental role in the understanding of the efficient photoisomerization, because of the possible efficient occurrence of $S_1(n\pi^*) \rightsquigarrow T_1(\pi\pi^*)$ intersystem crossing. The quantum efficiencies of the lowest triplet occupation are known to be relatively high for retinals (0.4–0.7) at room temperature in nonpolar solvents.[17] Moreover, the intersystem crossing efficiencies of retinals are considerably decreased in polar solvents, in accordance with the expected blueshift of the $n\pi^*$ state and the redshift of the $\pi\pi^*$ transition. The Franck–Condon triplet for the 11-*cis* isomer should be higher in energy than the *all-trans* conformer as a result of steric crowding, which can be assumed to be of the same order as the 11-*cis* ground state. It is qualitatively reproduced in the calculation and further confirmed employing the ground-state optimized 11-*cis* geometry. Notice that to build the potential energy curves the ground-state geometry of ATR was employed. For this reason, the 11-*cis* ground state is placed ≈ 1 eV higher. As a consequence the slope of the curves in the Φ interval from 0° to 90° is high. In the interval 0°–90°, the potential energy curves have been also computed employing the ground-state 11-*cis* geometry. The 11-*cis* ground state is then located at 0.25 eV above the *all-trans*, in accordance with the previous estimate at the HF level (see Sec. III A). The excited states suffer a proportional decrease at 0°. The S_0 state at 90° computed with the 11-*cis* geometry is located at higher energy than when calculated with the ATR ground-state geometry, which is below the Franck–Condon location of 11-*cis* T_1. Thus, even if the slope of the curves from 0° to 90° is not so pronounced in the lowest-energy path as shown in Fig. 2, the qualitative trends are maintained. The 11-*cis* T_1 can subsequently relax to 11-*cis* S_0 or to *trans* T_1. Efficient one-way isomerization along the T_1 surface could be understood with a deep well around the *trans* structure. Otherwise, if there was a T_1 potential minimum at the perpendicular conformation, it would cause efficient relaxation to S_0 at this position, leading to both ground-state *cis* and *trans*, contradicting experimental evidence. As shown in Fig. 2, perpendicular T_1 and *trans* T_1 are nearly isoenergetic. It also holds at the CASPT2 level, with a difference between them of only 0.1 eV. We have to recall that Fig. 2 represents simply a cut of a complex hypersurface. Relaxation of other geometric parameters can be also important to determine the lowest-energy path along T_1. Determination of the optimal structure of the lowest $\pi\pi^*$ triplet state, as well as its relative energy with respect to ground-state *all-trans*, is particularly interesting. The relaxation energy from the Franck–Condon $T_1(\pi\pi^*)$ state to its optimal geometry can be predicted around 0.4–0.6 eV. That is, the difference between the best theoretical estimate on the vertical excitation energy (1.96 eV) and the 0–0 experimental data for the singlet–triplet transition for ATR (1.54 eV)[25] or for the UND system (1.37 eV).[30] The prediction is consistent with the relaxation energy computed for the $T_1(\pi\pi^*)$ state of the UND system, 0.77(0.67) eV at the CASSCF(CASPT2) level. It automatically leads to a well-defined minimum around $\Phi = 180°$ along the T_1 hypersurface. The T_1 state may eventually relax to the ground-state S_0 *all-trans*-retinal.

The lowest path along the triplet hypersurface can be delineated as an energy surface descending from 11-*cis* T_1 to *all-trans* T_1 passing through a perpendicular conformation. The *all-trans* to 11-*cis* along the triplet surface is hindered by the shape of the potential energy surface, which enables instead an efficient relaxation to the ground state of *all-trans*-retinal.

IV. SUMMARY AND CONCLUSIONS

In this paper, we have presented results for the vertical excitation energies and properties on the low-lying excited states of *all-trans*-retinal, which are particularly relevant for the understanding of possible photoisomerization mechanisms. The calculations involve geometry optimizations for the ground state. The present results for the ground state are in agreement with the experimental crystal data, expect for certain bond lengths which are predicted somewhat longer in gas phase. It is probably due to both, puckering disorder in the crystal and certain underestimation of double bonds distances intrinsic to the x-ray technique.

Vertical excitation energies using the optimized ground state geometry have been computed for four singlet excited states and two triplet states with the CASSCF/CASPT2 method. The results obtained for *all-trans*-retinal, together with an extended treatment performed on its truncated model 3-methyl-*all-trans*(10-*s-cis*)-2,4,6,8,10-undecapentaen-1-al, show that the lowest singlet excited state has $n\pi^*$ character. The lowest triplet state is, however, described by the singly excited configuration $\pi\pi^*$. The most intense feature of the spectrum corresponds to the expected B_u-like transition of polyenes. The computed dipole moment for the state (≈ 8 D) confirms previous experimentally derived gas-phase data. The best estimate for the vertical A_g-like state places it close to the B_u-like state. The present theoretical description of the states is consistent with experimental evidence, except for the placement of the A_g-like state. It is vertically computed ≈ 1 eV higher than the maximum observed in the two-photon absorption spectra in solution. Based on previous experience on related systems and the magnitude of the calculated dipole moments, such deviation is suggested to be related to the nonvertical nature of the observed band in the two-photon absorption spectra, in addition to the influence of solvent effects.

Qualitative aspects on the 11-*cis* into *all-trans*-retinal photoisomerization have also been considered. The overall

scheme agrees with the initial transition to the *cis* $\pi\pi^*$ state, which will carry most of the energy. After radiationless transition to the $S_1(n\pi^*)$ state, efficient intersystem crossing to the *cis* $T_1(\pi\pi^*)$ state may occur. Descending from this point, passing through a perpendicular conformation, the *all-trans* $T_1(\pi\pi^*)$ minimum can be reached. A subsequent intersystem crossing may eventually lead to *all-trans*-retinal S_0. The present theoretical estimate gives therefore support to the previous experimentally deduced one-way photoisomerization mechanism, which has been demonstrated to take place mainly in the triplet manifold.

A generic prototype system undergoing photoisomerization can be denoted by RHC=CHR′, where depending on the meaning of R and R', key systems as retinal, stilbene, etc., can be built. The preferential photoisomerization mechanism is ultimately driven by the nature of the low-lying excited states and their relative energies on a complex multidimensional energy surface. In order to properly describe the lowest energy path, flexible wave functions including correlation effects are required. The CASSCF/CASPT2 method has proven to be a powerful tool. We have in the present work given one more illustration of its potential. Larger one-electron basis sets should, however, be employed to characterize quantitatively the static aspects of the considered isomerization process. Owing to the size of the retinal system, such study has to wait for further development of the computational methods.

ACKNOWLEDGMENTS

The research reported in this communication has been supported by the DGICYT project No. PB94-0986 of Spain. The latest stage of this work has been performed within the framework of the European Commission TMR network contract ERB FMRX-CT96-0079 (Quantum Chemistry of the Excited State). The authors thank Dr. B. O. Roos and Dr. A. R. de Lera for helpful discussions. Technical assistance by W. Díaz is also gratefully acknowledged.

[1] M. Ottolenghi, Adv. Photochem. **12**, 97 (1980).
[2] R. S. Becker, Photochem. Photobiol. **48**, 369 (1988).
[3] R. R. Birge, Annu. Rev. Phys. Chem. **41**, 683 (1990).
[4] Y. Koyama and Y. Mukai, Adv. Spectrosc. Biomol. Spectros. **21**, 49 (1993).
[5] G. Wald, Science **162**, 230 (1968).
[6] R. W. Schoenlein, L. A. Peteanu, R. A. Mathies, and C. V. Shank, Science **254**, 412 (1991).
[7] C. E. Randall, J. W. Lewis, S. J. Hug, S. C. Björling, I. Eisner-Shanas, N. Friedman, M. Ottolenghi, M. Sheves, and D. S. Kliger, J. Am. Chem. Soc. **113**, 3473 (1991).
[8] K. Nakanishi, A.-H. Chen, F. Derguini, P. Franklin, S. Hu, and J. Wang, Pure Appl. Chem. **66**, 981 (1994).
[9] R. R. Birge, D. F. Bocian, and L. M. Hubbard, J. Am. Chem. Soc. **104**, 1196 (1982).
[10] B. Honig, U. Dinur, R. R. Birge, and T. G. Ebrey, J. Am. Chem. Soc. **102**, 488 (1980).
[11] Y. Zhu, S. Ganapathy, A. Trehan, A. E. Asato, and R. S. H. Liu, Tetrahedron **48**, 10061 (1992).
[12] L. Serrano-Andrés, M. Merchán, I. Nebot-Gil, R. Lindh, and B. O. Roos, J. Chem. Phys. **98**, 3151 (1993).
[13] L. Serrano-Andrés, R. Lindh, B. O. Roos, and M. Merchán, J. Phys. Chem. **97**, 9360 (1993).
[14] M. Merchán and B. O. Roos, Theor. Chim. Acta **92**, 227 (1995).
[15] M. Merchán, B. O. Roos, R. McDiarmid, and X. Xing, J. Chem. Phys. **104**, 1791 (1996).
[16] T. Takemura, P. K. Das, G. Hug, and R. S. Becker, J. Am. Chem. Soc. **100**, 2626 (1978).
[17] P. K. Das and R. S. Becker, J. Am. Chem. Soc. **101**, 6348 (1979).
[18] T. Tahara and H. Hamaguchi, Chem. Phys. Lett. **234**, 275 (1995).
[19] J. D. Corsetti and B. E. Kohler, J. Chem. Phys. **67**, 5237 (1977).
[20] R. R. Birge, J. A. Bennett, L. M. Hubbard, H. L. Fang, B. M. Pierce, D. S. Kliger, and G. E. Leroi, J. Am. Chem. Soc. **104**, 2519 (1982).
[21] S. Alex, H. Le Thanh, and D. Vocelle, Can. J. Chem. **70**, 880 (1992).
[22] G. Drikos, H. Rüppel, W. Sperling, and P. Morys, Photochem. Photobiol. **40**, 85 (1984).
[23] G. Drikos and H. Rüppel, Photochem. Photobiol. **40**, 93 (1984).
[24] G. Drikos, P. Morys, and H. Rüppel, Photochem. Photobiol. **40**, 133 (1984).
[25] R. A. Raubach and A. V. Guzzo, J. Phys. Chem. **75**, 983 (1971).
[26] M. Ros, M. A. Hogenboom, P. Kok, and E. J. J. Groenen, J. Phys. Chem. **96**, 2975 (1992).
[27] E. J. J. Groenen, P. Kok, and M. Ros, Pure Appl. Chem. **64**, 833 (1992).
[28] Y. Mukai, H. Hashimoto, and Y. Koyama, J. Phys. Chem. **94**, 4042 (1990).
[29] Y. Mukai, M. Abe, Y. Katsuta, S. Tomozoe, M. Ito, and Y. Koyama, J. Phys. Chem. **99**, 7160 (1995).
[30] D. F. Evans. J. Chem. Soc. **1960**, 1735.
[31] R. S. Becker, P. K. Das, and G. Kogan, Chem. Phys. Lett. **67**, 463 (1979).
[32] T. Arai and K. Tokumaru, Chem. Rev. **93**, 23 (1993).
[33] H. Hamaguchi, H. Okamoto, M. Tasumi, Y. Mukai, and Y. Koyama, Chem. Phys. Lett. **107**, 355 (1984).
[34] H. Hamaguchi, J. Mol. Struc. **126**, 125 (1985).
[35] Y. Mukai, Y. Koyama, Y. Hirata, and N. Mataga, J. Phys. Chem. **92**, 4649 (1988).
[36] S. Ganapathy and R. S. H. Liu, J. Am. Chem. Soc. **114**, 3459 (1992).
[37] T. Tahara, B. N. Toleutaev, and H. Hamaguchi, J. Chem. Phys. **100**, 786 (1994).
[38] N.-H. Jensen, R. Wilbrandt, and R. V. Bensasson. J. Am. Chem. Soc. **111**, 7877 (1989).
[39] E. Hendrickx, K. Clays, A. Persoons, C. Dehu, and J. L. Brédas, J. Am. Chem. Soc. **117**, 3547 (1995).
[40] L. J. Weimann, G. M. Maggiora, and P. E. Blatz, Int. J. Quantum Chem. Quantum Biol. Symp. **2**, 9 (1975).
[41] B. O. Roos, in *Advances in Chemical Physics; Ab Initio Methods in Quantum Chemistry–II*, edited by K. P. Lawley (Wiley, Chichester, 1987), Chap. 69, p. 399.
[42] K. Andersson, P.-Å. Malmqvist, B. O. Roos, A. J. Sadlej, and K. Wolinski, J. Phys. Chem. **94**, 5483 (1990).
[43] K. Andersson, P.-Å. Malmqvist, and B. O. Roos, J. Chem. Phys. **96**, 1218 (1992).
[44] B. O. Roos, M. P. Fülscher, Per-Åke Malmqvist, M. Merchán, and L. Serrano-Andrés, in *Quantum Mechanical Electronic Structure Calculations with Chemical Accuracy*, edited by S. R. Langhoff (Kluwer Academic, Dordrecht, 1995), p. 357.
[45] B. O. Roos, K. Andersson, M. P. Fülscher, P.-Å. Malmqvist, L. Serrano-Andrés, K. Pierloot, and M. Merchán, in *Advances in Chemical Physics: New Methods in Computational Quantum Mechanics*, edited by S. A. Rice (Wiley, New York, 1995), Chap. XCIII, p. 219.
[46] L. Serrano-Andrés, B. O. Roos, and M. Merchán, Theor. Chim. Acta **87**, 387 (1994).
[47] B. O. Roos, M. Merchán, R. McDiarmid, and X. Xing, J. Am. Chem. Soc. **116**, 5927 (1994).
[48] M. J. Frisch, G. W. Trucks, H. B. Schlegel, P. M. W. Gill, B. G. Johnson, M. A. Robb, J. R. Cheeseman, T. Keith, G. A. Petersson, J. A. Montgomery, K. Raghavachari, M. A. Al-Laham, V. G. Zakrzewski, J. V. Ortiz, J. B. Foresman, J. Cioslowski, B. B. Stefanov, A. Nanayakkara, M. Challacombe, C. Y. Peng, P. Y. Ayala, W. Chen, M. W. Wong, J. L. Andres, E. S. Replogle, R. Gomperts, R. L. Martin, D. J. Fox, J. S. Binkley, D. J. Defrees, J. Baker, J. P. Stewart, M. Head-Gordon, C. Gonzalez, and J. A. Pople, GAUSSIAN 94, Revision B.1, Gaussian, Inc., Pittsburgh, 1995.
[49] B. O. Roos and K. Anderson, Chem. Phys. Lett. **245**, 215 (1995).
[50] P.-Å. Malmqvist, Int. J. Quantum Chem. **30**, 479 (1986).
[51] P. Å. Malmqvist and B. O. Roos, Chem. Phys. Lett. **155**, 189 (1989).
[52] K. Pierloot, B. Dumez, P.-O. Widmark, and B. O. Roos, Theor. Chim. Acta **90**, 87 (1995).
[53] K. Andersson, M. P. Fülscher, G. Karlström, R. Lindh, P.-Å. Malmqvist,

J. Olsen, B. O. Roos, A. J. Sadlej, M. R. A. Blomberg, P. E. M. Siegbahn, V. Kellö, J. Noga, M. Urban, and P.-O. Widmark, MOLCAS Version 3 (Dept. of Theor. Chem., Chem. Center, Univ. of Lund, P.O.B. 124, S-221 00 Lund, Sweden, Lund, 1994).
[54] M. P. Fülscher and B. O. Roos, Theor. Chim. Acta **87**, 403 (1994).
[55] M. Rubio, M. Merchán, E. Ortí, and B. O. Roos, Chem. Phys. **179**, 395 (1994).
[56] L. Serrano-Andrés, M. Merchán, I. Nebot-Gil, B. O. Roos, and M. P. Fülscher, J. Am. Chem. Soc. **115**, 6184 (1993).
[57] P. Du and E. R. Davidson, J. Phys. Chem. **94**, 7013 (1990).
[58] R. D. Gilardi, I. L. Karle, and J. Karle, Acta Cryst. **B 28**, 2605 (1972).
[59] T. Hamanaka, T. Mitsui, T. Ashida, and M. Kakudo, Acta Cryst. **B 28**, 214 (1972).
[60] J. H. Ippel, M. B. Spijker-Assink, M. Groesbeek, R. van der Steen, C. Altona, and J. Lugtenburg, Recl. Trav. Chim. Pays-Bas **113**, 99 (1994).
[61] A. R. de Lera, B. Iglesias, J. Rodríguez, R. Alvarez, S. López, X. Villanueva, and E. Padrós, J. Am. Chem. Soc. **117**, 8220 (1995).
[62] L. H. Scharpen, J. E. Wollrab, and D. P. Ames, J. Chem. Phys. **49**, 2368 (1968).
[63] M. Ponder and R. Mathies, J. Phys. Chem. **87**, 5090 (1983).
[64] L. Salem, Acc. Chem. Res. **12**, 87 (1979).
[65] L. Salem, *Electrons in Chemical Reactions: First Principles* (Wiley, New York, 1982).
[66] R. S. Mulliken, Phys. Rev. **41**, 751 (1932).
[67] N. J. Turro, *Molecular Photochemistry* (Benjamin, New York, 1965).